8-26-2022

Decentralized disturbance observer-based sliding mode load frequency control in multiarea interconnected power systems

Farhad Farivar
Edith Cowan University, f.farivar@ecu.edu.au

Octavian Bass
Edith Cowan University, o.bass@ecu.edu.au

Daryoush Habibi
Edith Cowan University, d.habibi@ecu.edu.au

10.1109/ACCESS.2022.3201873
Farivar, F., Bass, O., & Habibi, D. (2022). Decentralized disturbance observer-based sliding mode load frequency control in multiarea interconnected power systems. IEEE Access, 10, 92307-92320. https://doi.org/10.1109/ACCESS.2022.3201873

IEEE Access
Multidisciplinary ⋮ Rapid Review ⋮ Open Access Journal

Received 20 July 2022, accepted 15 August 2022, date of publication 26 August 2022, date of current version 8 September 2022.

Digital Object Identifier 10.1109/ACCESS.2022.3201873

RESEARCH ARTICLE

Decentralized Disturbance Observer-Based Sliding Mode Load Frequency Control in Multiarea Interconnected Power Systems

FARHAD FARIVAR, (Graduate Student Member, IEEE), OCTAVIAN BASS, (Senior Member, IEEE), AND DARYOUSH HABIBI, (Senior Member, IEEE)
School of Engineering, Edith Cowan University (ECU), Joondalup, Perth, WA 6027, Australia
Corresponding author: Farhad Farivar (f.farivar@ecu.edu.au)

ABSTRACT The load frequency control (LFC) problem in interconnected multiarea power systems is facing more challenges due to increasing uncertainties caused by the penetration of intermittent renewable energy resources, random changes in load patterns, uncertainties in system parameters and unmodeled system dynamics, leading to a compromised reliability of power systems and increasing the risk of power outages. In responding to this problem, this paper proposes a decentralized disturbance observer-based sliding mode LFC scheme for multiarea interlinked power systems with external disturbances. First, a reduced power system order is constructed by lumping disturbances from tie-line power deviations, load variations and the output power from renewable energy resources. The disturbance observer is then designed to estimate the lumped disturbance, which is further utilized to construct a novel integral-based sliding surface. The necessary and sufficient conditions to determine the tuning parameters of the sliding surface are then formulated in terms of linear matrix inequalities (LMIs), thus guaranteeing that the resultant sliding mode dynamics meet the H_∞ performance requirements. The sliding mode controller is then synthesized to drive the system trajectories onto the predesigned sliding surface in finite time in the presence of a lumped disturbance. From a practical perspective, the merit of the proposed control method is to minimize the impact of the lumped disturbance on the system frequency, which has not been considered to date in sliding mode LFC design. Numerical simulations are illustrated to validate the effectiveness of the proposed LFC strategy and verify its advantages over other approaches.

INDEX TERMS Load frequency control, renewable energy resources, sliding mode control, H_∞ control, linear matrix inequality.

I. INTRODUCTION

In recent years, LFC in multiarea interconnected power systems has experienced more challenges due to the penetration of intermittent renewable energy resources and changes in electricity consumption patterns [1]. In addition to uncertainties in system parameters, the fluctuating output power of renewable generators and random load changes have introduced more uncertainties to power systems; these uncertainties may cause significant frequency deviations [2]. In these environments, the main purpose of an LFC system is to maintain the power balance between the real and scheduled generation quantities for each area and to minimize tie-line power deviations between interlinked neighbouring areas [3]. A wide range of energy management strategies and control techniques have been introduced to deal with the recent LFC problem. Energy storage devices with fast response time such as batteries and supercapacitors have been utilized to improve grid frequency performance [4]. However, the application of these storage devices is limited to a small range due to high installation and maintenance costs [5]. Additionally, the optimal sizing and placement of these energy storage

The associate editor coordinating the review of this manuscript and approving it for publication was Padmanabh Thakur.

devices is a complex optimization problem. The distributed controllable loads (DCLs) have been introduced as an alternative cost-effective energy management approach, but the power system uncertainties make selecting a practical control strategy for DCLs a challenging task [5], [6]. Therefore, new frequency control strategies are required for existing LFC systems to ensure that power system frequency deviations are maintained within a permissible range in the presence of various uncertainties.

Although traditional PI controllers have been broadly employed to deal with LFC problems, controller performance is significantly affected under various operating conditions caused by load changes, system uncertainties and exogenous disturbances [7], [8] for the following reasons: i) the tuning parameters of PI controllers are assumed to be constant, and the desired system response can be obtained only in the area near a nominal operating point for which the controller is designed [9]; ii) PI controllers lead to long settling times and large overshoots in the frequency's transient response and may result in steady-state errors in response to time-varying disturbances [10]. Various optimization methods have been employed for tuning the parameters of PI controllers to improve system performance under various disturbances [11], [12], [13]. To address the drawbacks of traditional PI controllers for LFC applications, a wide range of control strategies have been extensively applied; these strategies include optimal control [14], [15], [16], [17], [18], adaptive control [19], [20], [21], [22], [23], fuzzy control [24], [25], [26], [27], [28], model-predictive control [29], [30], [31], [32], H_∞ control [2], [33], [34], [35], [36], and variable structure control [37], [38], [39], [40], [41]. A broad literature review on the effectiveness of various control strategies for the LFC can be found in [17], [42], and [43].

SMC, as a variable structure control method, has recently attracted the attention of researchers in LFC problems due to its striking features, such as high transient performance and robustness against plant uncertainties [44], [45], [46], [47], [54]. In addition, many smart grid researchers have shown interest in studying SMC-based load frequency controllers in interconnected power systems with communication delays [55], [56], [57]. Although traditional SMC is robust against matched disturbances [48], it cannot effectively attenuate mismatched load disturbances entering the system through points other than the control input. These mismatched disturbances not only affect system state variables directly but also increase chattering problems and severely degrade the performance of the sliding surface in traditional SMC, thereby weakening the inherent robustness of SMC [49]. Accordingly, designing an effective sliding surface to attenuate the impact of lumped mismatched disturbances on the LFC problem has received increasing attention in recent years. The authors of [50], [51], [52], and [53] considered the problem of mismatched load disturbances and parameter uncertainties in frequency controller design. In these works, all mismatched disturbances and uncertainties were lumped together, but under a restrictive assumption on the rank of the lumped disturbance matrix to retain the robustness of traditional SMC against mismatched disturbances. In addition, no systematic approach was employed to determine the unknown parameters of the sliding mode controller to guarantee the desired response. The authors of [6] designed a hybrid fuzzy logic nonlinear SMC in which the controller gains were tuned by deriving a novel imperialistic competitive algorithm and a continuous approximated function was suggested to handle the chattering problem.

As a practical alternative approach, several authors have considered disturbance observer-based SMC approaches for LFC problems to reduce the chattering problem and maintain nominal frequency controller performance. For instance, a discrete-time sliding mode load frequency controller based on a disturbance observer was introduced in [52], but the results showed that the chattering problem was not fully resolved because the estimation of aggregate disturbances was not directly involved in the sliding surface design. The proposed approach in [58] applied a disturbance observer in the controller design and introduced an optimal sliding manifold based on an LQR algorithm; this approach was robust against mismatched uncertainties and unmodeled dynamics. However, the approach was conservative, as the disturbance observer design was limited to tracking slow-varying step load disturbances, where the effectiveness of the approach against random disturbances was not investigated. The authors of [51] and [59] employed disturbance observer-based SMC frequency controllers, but no optimal method was utilized to determine unknown parameters of the sliding manifolds. Furthermore, the aforementioned approaches have not considered an upper bound limit for lumped disturbance estimation error, and thus do not systematically prove the disturbance estimation error to be sufficiently close to zero. The proposed disturbance observers in [51], [53], and [58] have been developed based on a conservative assumption that the first derivative of lumped disturbance is zero, thus degrading the dynamic performance of the system in tracking non-constant random lumped disturbance caused by intermittent renewable energy resources and complex load patterns. To our knowledge, none of the abovementioned sliding mode frequency controllers have straightforwardly incorporated the estimation of disturbances in the design of the sliding surface to compensate for mismatched disturbances. This approach helps maintain the nominal performance of a system and alleviates chattering problems. Although reports of the aforementioned approaches have claimed that the effect of lumped disturbance on the frequency deviations has been reduced, the impact of minimizing disturbances on system frequency has not been addressed in control objectives. From a practical point of view in relation to LFC problems, it is important to minimize the effects of lumped disturbances on system frequency deviations straightforwardly.

NOMENCLATURE

i	Subscript referring to area i.
j	Subscript referring to area j .
Δf_i	Deviation in frequency (Hz).
ΔX_{G_i}	Deviation in governor valve position (p.u.MW).
ΔP_{G_i}	Deviation in generator output (p.u.MW).
ΔP_{D_i}	Accumulated external disturbance from load and renewables (p.u.MW).
ΔP_{L_i}	Deviation in load disturbance (p.u.MW).
ΔP_{R_i}	Deviation in renewable energy resource output power disturbance (p.u.MW).
ΔP_{T_i}	Tie line power flow (p.u.MW).
ΔD_{T_i}	Deviation in tie-line power flow (p.u.MW).
T_{P_i}	Power system time constant (sec).
T_{T_i}	Turbine time constant (sec).
T_{G_i}	Governor time constant (sec).
K_{P_i}	Power system gain (Hz/p.u.MW).
T_{ij}	Tie-line synchronization gain between area i and j (p.u.MW/rad/sec).
R_i	Droop coefficient (Hz/p.u.MW).
$B^{\dagger}$	Pseudo inverse of matrix B.
$B^{\perp}$	Orthogonal complement of matrix B.
$*$	Transposed elements of a symmetrical matrix.
PI	Proportional integral.
LQR	Linear quadratic regulator.
SMC	Sliding mode control.
DOB	Disturbance observer-based.
LFC	Load frequency control.
SMLFC	Sliding mode load frequency control.
LMI	Linear matrix inequality.
GRC	Generation rate constraint p.u.MW/sec.
GDB	Governor deadband.

In this paper, a decentralized disturbance observer-based SMC approach is proposed to address LFC problems of multiarea power systems with mismatched disturbances and uncertainties from the load and generation sides. Motivated by the above literature review, the contributions of this work are as follows:

- A disturbance observer is designed to estimate the lumped disturbance, including system parameter uncertainties, load variation, renewable output power fluctuations and tie-line power flow deviations.
- The conservatism of the proposed approaches in [51], [53], and [58] is relaxed by considering an upper bound limit for the lumped disturbance and its first derivative. It is demonstrated that the lumped disturbance estimation error remains sufficiently close to a small neighbourhood of zero at all times. This is an important practical consideration for estimating non-constant lumped disturbance.
- Based on the estimation of disturbances, a novel integral sliding surface is proposed in which the solvability condition to determine the tuning parameter of the proposed sliding surface is transferred into the problem of designing an H_∞ state feedback controller for sliding mode dynamics. From a practical point of view, this technique has the advantage of minimizing the impact of lumped disturbance on frequency deviations (controlled output).
- An LMI-based optimization algorithm is derived to determine the tuning parameter of the sliding surface to ensure that the resultant sliding mode dynamics meet the H_∞ performance requirements. Note that the proposed LMI is constructed by adding slack variables to relax feasibility conditions and reduce the inherent conservatism of the control strategies in [34], [60], [61], [62], [63], and [64].
- A sliding mode controller is synthesized to drive the system trajectories onto a region near the predesigned sliding surface in finite time in the presence of a lumped disturbance and to maintain them therein afterward. The proposed controller has the advantage of low computational burden for practical implementations.

The remaining sections of this paper are structured as follows. Section 2 describes the dynamic model of a multiarea power system for the LFC problem. Section 3 demonstrates the design of the disturbance observer. The sliding mode frequency controller is synthesized in Section 4. Section 5 presents simulation results for different scenarios to verify the feasibility and effectiveness of the proposed approach for the LFC problem. Conclusions and discussion of possible future work can be found in Section 6.

II. DYNAMIC MODEL OF A MULTIAREA POWER SYSTEM

It has been well established that a multiarea power system is a coupled nonlinear system that is exposed to parametric uncertainties and exogenous disturbances. However, a linearized power system model can be used for studying LFC problems due to slow changes in loads and resources during normal operations [3], [7]. A conventional decentralized LFC model for the ith area of a multiarea power system is depicted in Fig. 1.

The governing equations of the system dynamics for the ith area are given as follows:

$$\Delta\dot{f}_i(t) = -\frac{1}{T_{P_i}(t)}\Delta f_i(t) + \frac{K_{P_i}(t)}{T_{P_i}(t)}\Delta P_{G_i}(t) - \frac{K_{P_i}(t)}{T_{P_i}(t)} \times \Delta P_{D_i}(t) - \frac{K_{P_i}(t)}{T_{P_i}(t)}\Delta P_{T_i}(t) \tag{1}$$

$$\Delta\dot{P}_{G_i}(t) = \frac{1}{T_{T_i}(t)}\Delta X_{G_i}(t) - \frac{1}{T_{T_i}(t)}\Delta P_{G_i}(t) \tag{2}$$

$$\Delta\dot{X}_{G_i}(t) = \frac{1}{T_{G_i}(t)}u_i(t) - \frac{1}{R_i T_{G_i}(t)}\Delta f_i(t) - \frac{1}{T_{G_i}(t)}\Delta X_{G_i}(t) \tag{3}$$

$$\Delta\dot{P}_{T_i}(t) = 2\pi\sum_{\substack{j=1\\ j\neq i}}^{N} T_{ij}(\Delta f_i(t) - \Delta f_j(t)) \tag{4}$$

$$y_i(t) = \Delta f_i(t) \tag{5}$$

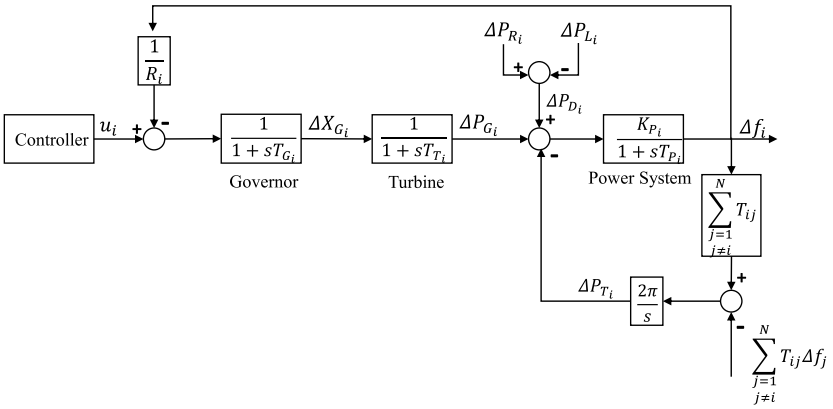

FIGURE 1. Multiarea power system: LFC scheme of *i*th area [58].

Since the main aim of LFC is to maintain frequency deviations within permissible limits, the controller must guarantee a suitable signal to the generator output to generate the following variations in the load and tie-line power. Thus, $\Delta P_{T_i}(t)$ can be treated as a bounded external disturbance for the ith area [58]; this disturbance can be added to the external disturbance $\Delta P_{D_i}(t)$ in the i*th* area to determine the total external disturbance $\Delta D_i(t) = \Delta P_{D_i}(t) + \Delta P_{T_i}(t)$. Note that the aggregate disturbance $\Delta D_i(t)$ is assumed to satisfy the condition $|\Delta D_i(t)| \leqslant \alpha_i$ in which α_i is a positive constant. Based on this notion, a new reduced-order model of the system dynamics can be derived by inserting the integral of (4) into (1) and substituting the result into (2) and (3), which is represented in the following state space form:

$$\begin{aligned} \dot{x}_i(t) &= A_i(t)x_i(t) + B_i(t)u_i(t) + H_i(t)\Delta D_i(t) \\ y_i(t) &= C_i x_i(t) \end{aligned} \tag{6}$$

where $x_i \in R^n$ is the system state vector as $x_i(t) = [\Delta f_i(t) \quad \Delta P_{G_i}(t) \quad \Delta X_{G_i}(t)]^T$, $u_i \in R$ is the control input, the aggregate disturbance is $\Delta D_i(t)$ and the controlled output is $y_i(t)$. The system matrices $A_i(t), B_i(t), H_i(t)$ and C_i are real matrices with appropriate dimensions, which are given as follows:

$$A_i(t) = \begin{bmatrix} -\frac{1}{T_{P_i}(t)} & \frac{K_{P_i}(t)}{T_{P_i}(t)} & 0 \\ 0 & -\frac{1}{T_{T_i}(t)} & \frac{1}{T_{T_i}(t)} \\ -\frac{1}{R_i T_{G_i}(t)} & 0 & -\frac{1}{T_{G_i}(t)} \end{bmatrix}$$

$$Bi(t) = \begin{bmatrix} 0 & 0 & \frac{1}{T_{G_i}(t)} \end{bmatrix}^T$$

$$H_i(t) = \begin{bmatrix} -\frac{K_{P_i}(t)}{T_{P_i}(t)} & 0 & 0 \end{bmatrix}^T$$

$$C_i = \begin{bmatrix} 1 & 0 & 0 \end{bmatrix}$$

The system model expressed in (6) can be rearranged as

$$\dot{x}_i(t) = (A_i + \Delta A_i(t))x_i(t) + (B_i + \Delta B_i(t))u_i(t) + (H_i + \Delta H_i(t))\Delta D_i(t), \tag{7}$$

where A_i,B_i and H_i represent the nominal parts of the system; and where $\Delta A_i(t)$, $\Delta B_i(t)$ and $\Delta H_i(t)$ are the uncertain matrices with limited bounds. By defining $d_i(t) = \Delta A_i(t)x_i(t) + \Delta B_i(t)u_i(t) + (H_i + \Delta H_i(t))\Delta D_i(t)$, (7) can be rewritten as

$$\dot{x}_i(t) = A_i x_i(t) + B_i u_i(t) + d_i(t) \tag{8}$$

Assumption 1: The disturbance $d_i(t)$ is supposed to meet the criteria $\|d_i(t)\| \leqslant d_i^*$ and $\left\|\dot{d}_i(t)\right\| \leqslant \dot{d}_i^*$, in which d_i^* and $\dot{d}_i^*$ are nonnegative constants.

Definition 1: Let γ be a given positive scalar. The open loop form of System (8) satisfies the H_∞ performance requirements if both of the following conditions are fulfilled:

1) For $d_i(t) = 0$, the corresponding system is stable.
2) $\forall d_i(t) \neq 0, \ t \in [0, \infty)$ and under zero initial condition,

$$\int_0^\infty \|y_i(t)\|^2 dt \leqslant \gamma^2 \int_0^\infty \|d_i(t)\|^2 dt.$$

The objective of this paper is to design a disturbance observer-based SMC for the LFC system given by (8) in such a way that 1) the reachability of the closed-loop system onto the proposed sliding surface is satisfied and 2) the resulting sliding mode dynamics meet the H_∞ performance requirements defined in Definition 1.

Remark 1: Note that the control objective is to stabilize the state trajectories of the controlled plant (8), meaning that both the state vectors $x_i(t)$ and the control input $u_i(t)$ are bounded, and since $\Delta D_i(t)$ is assumed to be bounded, $d_i(t)$ is concluded to be a bounded disturbance.

Remark 2: One of the practical limitations for the LFC problem is inability to measure all the external and internal disturbances. A realistic solution is to estimate all the disturbances by utilizing the defined lumped disturbance term.

III. DISTURBANCE OBSERVER DESIGN

In this section, a disturbance observer is designed to estimate the lumped disturbance in (8). The dynamic equation of the disturbance observer is expressed as follows:

$$\begin{aligned} \dot{p}_i(t) &= \Gamma_i \hat{d}_i(t) + \Gamma_i(A_i x_i(t) + B_i u_i(t)) \\ \hat{d}_i(t) &= p_i(t) - \Gamma_i x_i(t) \end{aligned} \tag{9}$$

where $p_i(t)$ is the state vector of the observer, $\hat{d}_i(t)$ is the estimate of $d_i(t)$ in (8), and Γ_i is a Hurwitz matrix. Combining (8) and (9) gives

$$\dot{\hat{d}}_i(t) = \Gamma_i(\hat{d}_i(t) - d_i(t)) \tag{10}$$

Defining the estimation error as $\tilde{d}_i(t) = d_i(t) - \hat{d}_i(t)$, (10) can be rewritten as

$$\dot{\tilde{d}}_i(t) = \dot{d}_i(t) + \Gamma_i\tilde{d}_i(t) \tag{11}$$

Accordingly, we have the following lemma regarding the boundedness of $\tilde{d}_i(t)$.

Lemma 1: There exists a bounded scalar λ_i such that the disturbance estimation error $\tilde{d}_i(t)$ satisfies $\left\|\tilde{d}_i(t)\right\| \leq \lambda_i$.

Proof: It can be verified that the solution of (11) is $\tilde{d}_i(t) = e^{\Gamma_i t}\tilde{d}_i(0) + \int_0^t e^{\Gamma_i(t-\tau)}\dot{d}_i(\tau)d\tau$, from which the following inequality holds:

$$\left\|\tilde{d}_i(t)\right\| \leqslant \left\|e^{\Gamma_i t}\tilde{d}_i(0)\right\| + \left\|\int_0^t e^{\Gamma_i(t-\tau)}\dot{d}_i(\tau)d\tau\right\| \tag{12}$$

We can use the bound $\left\|e^{\Gamma_i t}\right\| \leq \alpha_i e^{\lambda_{\max}(\Gamma_i)t}$ to estimate the solution by

$$\begin{aligned}\left\|\tilde{d}_i(t)\right\| &\leqslant \alpha e^{\lambda_{\max}(\Gamma_i)t}\left\|\tilde{d}_i(0)\right\| \\ &\quad + \int_0^t \alpha e^{\lambda_{\max}(\Gamma_i)(t-\tau)}\left\|\dot{d}_i(\tau)\right\| d\tau \\ &\leqslant \alpha e^{\lambda_{\max}(\Gamma_i)t}\left\|\tilde{d}_i(0)\right\| + \alpha(\sup_{0\leqslant\tau\leqslant t}\left\|\dot{d}_i(\tau)\right\|) \\ &\quad \times \int_0^t e^{\lambda_{\max}(\Gamma_i)(t-\tau)}d\tau \\ &\leqslant \alpha\left\|\tilde{d}_i(0)\right\| - \frac{\alpha}{\lambda_{\max}(\Gamma_i)}(\sup_{0\leqslant\tau\leqslant t}\left\|\dot{d}_i(\tau)\right\|) \triangleq \lambda_i\end{aligned}$$

In accordance with Assumption 1, $\left\|\dot{d}_i(t)\right\| \leqslant \dot{d}_i^*$. Therefore, λ_i is bounded, and the proof is completed. ■

Remark 3: From a practical point of view, the upper bound of $\tilde{d}_i(t)$ is to be a small value to guarantee the performance of the designed disturbance observer. Thus, it is an important design consideration that the absolute value of the largest eigenvalue of the matrix Γ_i must be large enough to minimize λ_i.

IV. SYNTHESIS OF THE SLIDING MODE LOAD FREQUENCY CONTROLLER

This section addresses the design of a sliding mode controller for the problem of frequency deviation in multiarea power systems as described by (8). The objective is to analyze sliding mode dynamics with bounded $\mathcal{L}_2$-gain performance. In this section, an integral sliding surface is proposed based on the disturbance estimation d_i(t). A sliding mode control law is then constructed to reject the lumped disturbance so that the reachability of the sliding surface is guaranteed. Finally, an H_∞-based control strategy is employed to determine the controller and disturbance observer gains. The structure of the proposed controller is shown in Fig. 2.

Consider the following disturbance observer-based integral sliding surface:

$$\begin{aligned}S_i(t) &= G_i(x_i(t) - x_i(0) \\ &\quad - \int_0^t (A_i x_i(\tau) + B_i u_{N_i}(\tau) + \hat{d}_i(\tau))d\tau\end{aligned} \tag{13}$$

where $G_i \in R^{m\times n}$ is to be selected to satisfy $G_iB_i = I_n$. Since B_i is of full column rank, G_i can be chosen as $B_i^\dagger$, and $u_{N_i}(t) = -K_ix_i(t) - G_i\hat{d}_i(t)$, in which K_i is designed such that the sliding mode dynamics meet the required control objectives defined later.

Remark 4: The advantage of the proposed sliding surface (13) over traditional sliding surfaces is the use of $\hat{d}_i(t)$ to actively reduce the impacts of the unknown disturbance $d_i(t)$.

Let us assume that K_i is a known parameter. The next theorem shows that the state trajectories of System (8) reach the sliding surface $S_i(t) = 0$ by applying the control law as

$$u_i(t) = u_{N_i}(t) + G_iu_{M_i}(t) \tag{14}$$

where $u_{M_i}(t) = -(\rho_i + \lambda_i)\, sgn(G_i^T S_i(t))$, $\rho_i > 0$.

Theorem 1: The reachability of the sliding surface $S_i(t) = 0$ is guaranteed in finite time by employing the controller (14)

Proof: With $V_i(t) = \frac{1}{2}S_i^T(t)S_i(t)$ as a Lyapunov function candidate, we obtain

$$\begin{aligned}\dot{V}_i(t) &= S_i^T(t)G_i\left(A_ix_i(t) + B_iu_i(t) + d_i(t)\right. \\ &\quad \left. - \left(A_ix_i(t) + B_iu_{N_i}(t) + \hat{d}_i(t)\right)\right) \\ &= S_i^T(t)G_i\left(B_i\left(u_i(t) - u_{N_i}(t)\right) + \left(d_i(t) - \hat{d}_i(t)\right)\right) \\ &= S_i^TG_i\left(u_{M_i}(t) + \tilde{d}_i(t)\right)\end{aligned} \tag{15}$$

Substituting $u_i(t)$ from (14) into (15), we obtain

$$\begin{aligned}\dot{V}_i(t) &= S_i^T(t)G_i\left(-(\rho_i + \lambda_i)\, sgn(G_i^TS_i(t)) + \tilde{d}_i(t)\right) \\ &= -(\rho_i + \lambda_i)\left\|S_i^T(t)G_i\right\| + S_i^TG_i\tilde{d}_i(t) \\ &\leqslant -\rho_i\left\|S_i^T(t)G_i\right\|\end{aligned}$$

Therefore, $\dot{V}_i(t) \leqslant 0$, and the reachability condition is achieved in finite time. This completes the proof. ■

Implementing the function $sgn(G_i^TS_i(t))$ may cause an undesirable chattering phenomenon. A practical solution is to replace this function with either a smooth function $tanh(G_i^TS_i(t))$ or a high slope saturation function $sat(G_i^TS_i(t))$ [70].

In the next step, an equivalent control law is utilized to determine the unknown parameter K_i of the sliding surface (13). By solving $\dot{S}_i(t) = 0$, the equivalent control law is obtained as $u_i^{eq}(t) = u_{N_i}(t) - G_i\tilde{d}_i(t)$. By substituting $u_i^{eq}(t)$ in (8), it can be verified that

$$\begin{aligned}\dot{x}_i(t) &= A_ix_i(t) + B_i(u_{N_i}(t) - G_i\tilde{d}_i(t)) + d_i(t) \\ &= (A_i - B_iK_i)x_i(t) - B_iG_id_i(t) + d_i(t)\end{aligned} \tag{16}$$

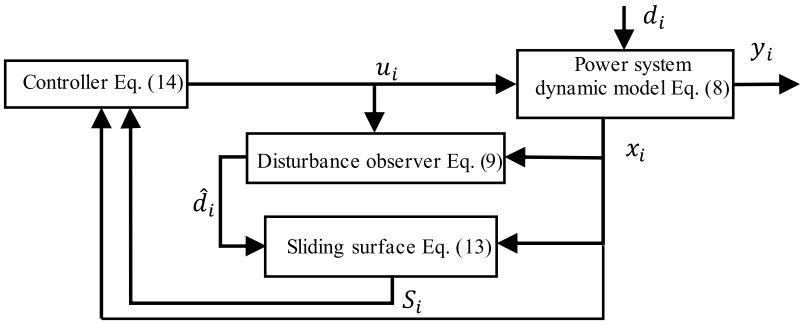

FIGURE 2. Structure of the proposed disturbance observer-based sliding mode load frequency controller for the *i*th area of the power system.

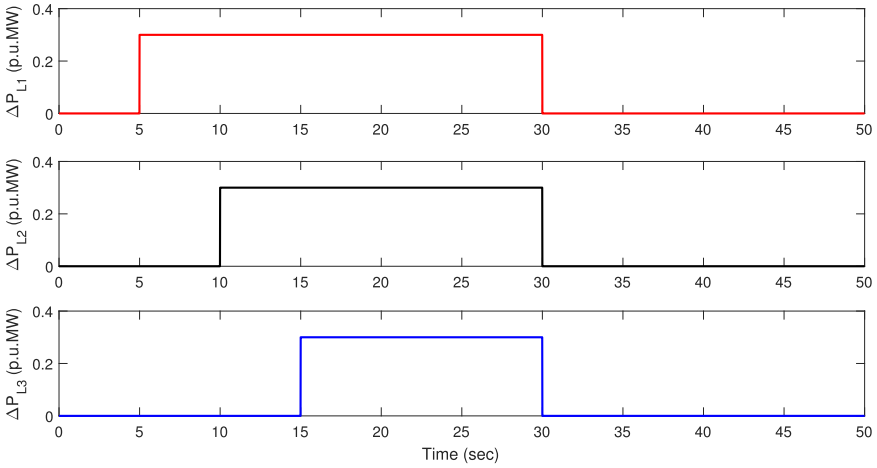

FIGURE 3. Step load disturbance.

Considering that $B_iG_i = I_n - B_i^{\perp}G_i^{\perp T}$, the sliding mode dynamics are obtained as follows:

$$\dot{x}_i(t) = (A_i - B_iK_i)x_i(t) + B_i^{\perp}G_i^{\perp T}d_i(t) \tag{17}$$

Defining $\tilde{G}_i = B_i^{\perp}G_i^{\perp T}$, we have

$$\dot{x}_i(t) = (A_i - B_iK_i)x_i(t) + \tilde{G}_id_i(t) \tag{18}$$

Furthermore, the control problem is to design the parameter K_i in (18) such that the sliding mode dynamics meet the H_∞ performance requirements given in Definition 1. To achieve this, an efficient LMI-based design approach will be proposed in the theorem below to determine the parameter appropriately. Before proceeding further, some useful lemmas are introduced, which will be required in proving the subsequent theorem.

Lemma 2 [65]: The system in (18) meets the H_∞ performance requirements if and only if there exists a positive-definite matrix P_i such that the following LMI holds:

$$\min_{K_i} \ \gamma_i$$
$$s.t \begin{bmatrix} {A_{cl_i}}^T P_i + P_i A_{cl_i} & P_i\tilde{G}_i & {C_i}^T \\ * & -\gamma_i I_2 & 0 \\ * & 0 & -\gamma_i I_2 \end{bmatrix} < 0 \tag{19}$$

where $A_{cl_i} = A_i - B_iK_i$. Note that by changing the second and third columns of (19) and in turn the corresponding second and third rows, the following equivalent condition can be obtained:

$$\min_{K_i} \ \gamma_i$$
$$s.t \begin{bmatrix} {A_{cl_i}}^T P + PA_{cl_i} & {C_i}^T & P\tilde{G}_i \\ * & -\gamma_i I_2 & 0 \\ * & 0 & -\gamma_i I_2 \end{bmatrix} < 0 \tag{20}$$

Lemma 3 [66]: Consider matrices Π, Φ and Ψ, and suppose $\Pi = \Pi^T$. The following two statements are equivalent:

$$\begin{aligned} &\text{I)}\ \Phi^{\perp}\Pi\ {\Phi^{\perp}}^T < 0, \quad {\Psi^T}^{\perp}\Pi\ {\Psi^T}^{\perp T} < 0, \\ &\text{II)}\ \Pi + \Phi\theta\Psi + (\Phi\theta\Psi)^T < 0, \end{aligned} \tag{21}$$

Theorem 2:

$$\min_{K_i} \ \gamma_i$$
$$s.t \begin{bmatrix} -Q_i - Q_i^T & * & * & * & * \\ A_iQ_i - B_iY_i + X_i & -X_i & * & * & * \\ C_iQ_i & 0 & -\gamma_i I & * & * \\ Q_i & 0 & 0 & -X_i & * \\ 0 & \tilde{G}_i^T & 0 & 0 & -\gamma_i I \end{bmatrix} < 0 \tag{22}$$

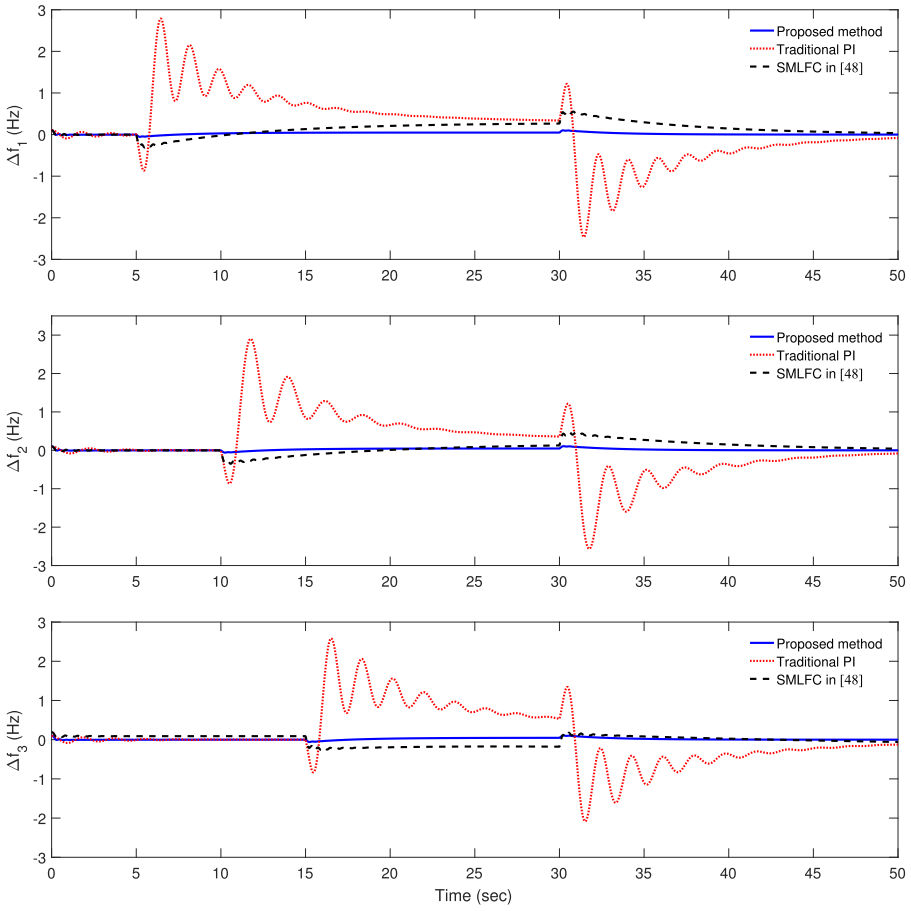

FIGURE 4. Comparative dynamic responses of the system frequency deviations Δf_i in all three areas.

In addition, if the condition (22) is feasible, the parameter K_i can be obtained as $K_i = Y_i Q_i^{-1}$

Proof: Define $X_i = P_i$. Left- and right-multiplying the constraint of the LMI (20) by $diag\{X_i, I_2, I_2\}$ and its transpose, respectively, and then applying the Schur complement results in

$$\begin{bmatrix} X_i {A_{cl_i}}^T + A_{cl_i} X_i + \frac{1}{\gamma_i}\tilde{G}_i\tilde{G}_i^T & X_i {C_i}^T \\ * & -\gamma_i I_2 \end{bmatrix} < 0 \qquad (23)$$

The Schur complement verifies that the above inequality is equivalent to

$$\begin{bmatrix} X_i {A_{cl_i}}^T + A_{cl_i} X_i - X_i + \frac{1}{\gamma_i}\tilde{G}_i\tilde{G}_i^T & X_i {C_i}^T & X_i \\ * & -\gamma_i I_2 & 0 \\ * & * & -X_i \end{bmatrix} < 0 \qquad (24)$$

If we choose the following matrix variables

$$\Pi = \begin{bmatrix} 0 & X_i & 0 & 0 & 0 \\ X_i & -X_i & 0 & 0 & 0 \\ 0 & 0 & -\gamma_i I_2 & 0 & 0 \\ 0 & 0 & 0 & X_i & 0 \\ 0 & 0 & 0 & 0 & \gamma_i I_2 \end{bmatrix}$$

$$\Phi = \begin{bmatrix} -I_9 & {A_{cl_i}}^T & {C_i}^T & I_9 & 0 \\ 0 & \tilde{G}_i^T & 0 & 0 & \gamma_i I_2 \end{bmatrix}$$

$$\Psi = \begin{bmatrix} I_9 & 0 & 0 & 0 & 0 \\ 0 & 0 & 0 & 0 & I_2 \end{bmatrix}$$

$$\Phi^{\perp} = \begin{bmatrix} A_{cl_i} & {C_i}^T & I_9 \\ I_9 & 0 & 0 \\ 0 & I_2 & 0 \\ 0 & 0 & I_9 \\ \frac{1}{\gamma_i}\tilde{G}_i^T & 0 & 0 \end{bmatrix}$$

$$\Psi^{\perp} = \begin{bmatrix} 0 & 0 & 0 \\ I_9 & 0 & 0 \\ 0 & I_2 & 0 \\ 0 & 0 & I_9 \\ 0 & 0 & 0 \end{bmatrix} \qquad (25)$$

it can be readily obtained that

$$\Phi^{\perp T}\Pi\Phi^{\perp} = \begin{bmatrix} X_i {A_{cl_i}}^T + A_{cl_i} X_i - X_i + \frac{1}{\gamma_i}\tilde{G}_i\tilde{G}_i^T & X_i {C_i}^T & X_i \\ * & -\gamma_i I & 0 \\ * & * & -X_i \end{bmatrix} < 0$$

$$\Psi^{\perp T}\Pi\Psi^{\perp}$$

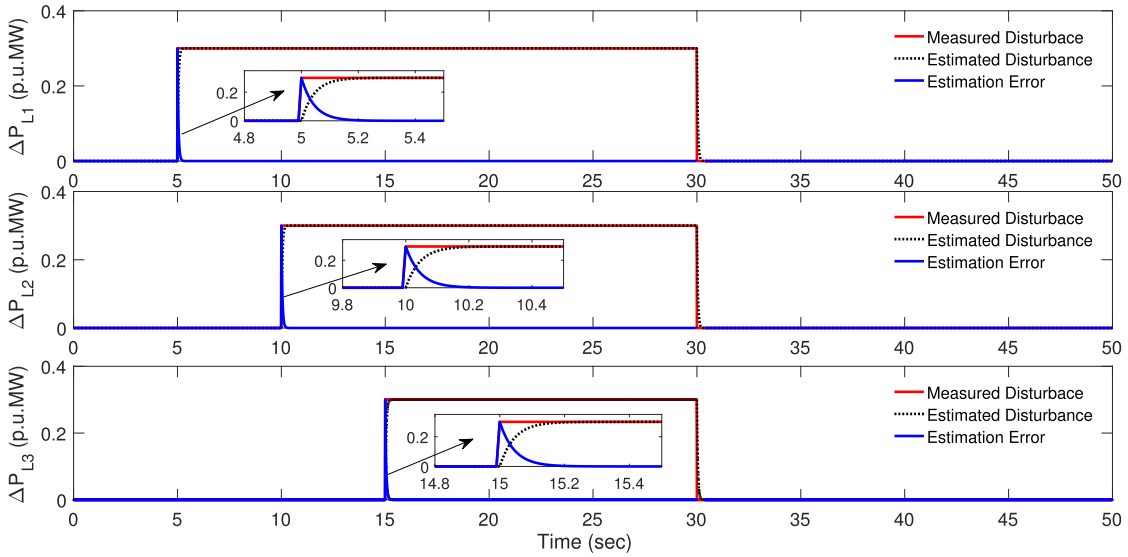

FIGURE 5. Dynamic response of the proposed disturbance observer and disturbance estimation error.

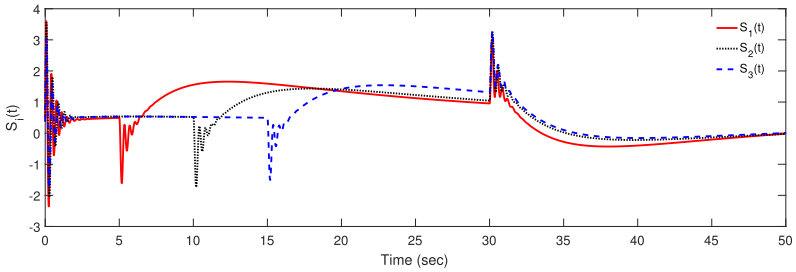

FIGURE 6. Sliding surface $S_i(t)$.

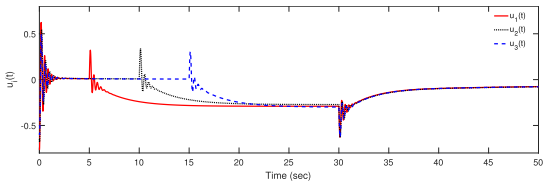

FIGURE 7. Control effort $u_i(t)$.

$$= \begin{bmatrix} -X_i & 0 & 0 \\ 0 & -\gamma_i I & 0 \\ 0 & 0 & -X_i \end{bmatrix} < 0 \tag{26}$$

Therefore, according to Lemma 3, there exists a matrix such that $\Pi + \Phi Q \Psi + (\Phi Q \Psi)^T < 0$. Substituting the matrix variables (25) in the above inequality and defining $Y_i = K_i Q_i$, the condition (22) is obtained. Furthermore, the (1, 1) element of (22) shows that $-Q_i - Q_i^T < 0$; therefore, Q_i is an invertible matrix. Hence, the parameter K_i is obtained as $K_i = Y_i Q_i^{-1}$. This completes the proof. ■

Remark 5: Note that condition (24) has the advantage of introducing the slack variables X_i and Q_i; therefore, the conservativeness of condition (22) is reduced compared to that of condition (20).

TABLE 1. Nominal parameters of the three-area power system [50].

Area	R_i	T_{G_i}	T_{T_i}	K_{P_i}	T_{P_i}	T_{ij}
1	2.4	0.08	0.3	120	20	0.55
2	2.7	0.072	0.33	112.5	25	0.65
3	2.5	0.07	0.35	115	20	0.545

V. SIMULATION RESULTS

To demonstrate the effectiveness of the proposed control scheme, three simulation scenarios are studied for a three-area interconnected thermal power system under different load perturbations, parameter uncertainties and renewable output power fluctuations. The nominal values for the three-area power system are given in Table 1. The tuning parameter of the disturbance observer for all areas is chosen as

$$\Gamma_i = \begin{bmatrix} -20 & 0 & 0 \\ 0 & -30 & 0 \\ 0 & 0 & -15 \end{bmatrix}$$

The tuning parameter ρ of the proposed controller (14) is selected as 0.1 for all three areas. YALMIP [67] is used to solve the LMI condition (22) to calculate the minimum value of the H_∞ performance $\gamma_i^{\min}$ and to determine the tuning

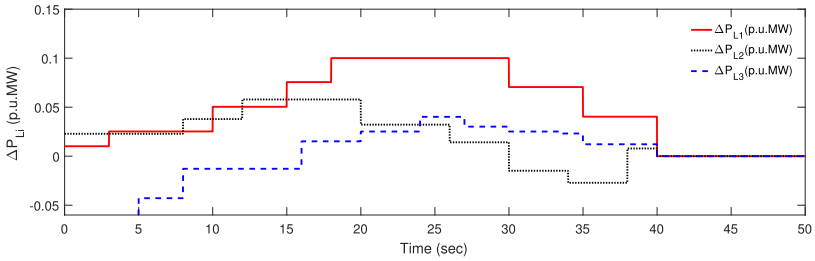

FIGURE 8. Time-varying step load disturbance profile in the *i*th area.

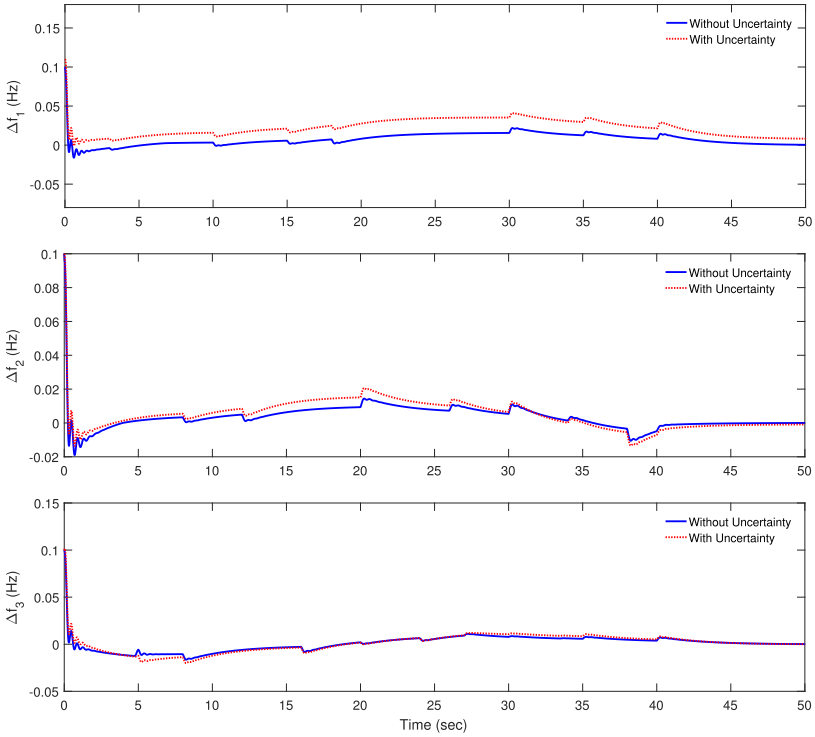

FIGURE 9. Dynamic response of the system frequency deviations Δf_i in all three areas with parameter uncertainties.

TABLE 2. H_∞ Performance index ${\gamma_i}^{\min}$ and tuning parameter of sliding surfaces for all three areas.

Area	${\gamma_i}^{\min}$	Sliding Surface Parameter K_i
1	0.4354	K_1=[7.6180 8.0106 -0.0969]
2	0.2123	K_2=[6.7164 5.8949 -0.2850]
3	0.3918	K_3=[6.0677 6.5940 -0.2248]

parameter of the sliding surface K_i in each area. A summary of the results is presented in Table 2.

Scenario 1: In this subsection, the proposed LFC strategy is tested for nominal power system parameters under relatively large step load perturbations applied to all three areas, as depicted in Fig. 3. A sudden step load increase of 0.3 p.u. occurs in Areas 1, 2 and 3 at $t = 5$ s, $t = 10$ s and $t = 15$ s, respectively. The system frequency deviation responses Δf_i, $i = 1, 2, 3$ of the proposed method in all three areas are compared with the conventional PI and SMLFC methods in [53], as shown in Fig. 4.

From the simulation results, the proposed approach outperforms the aforementioned approaches. Compared with the other two strategies, the scheme exhibits a better transient response in relation to overshoot, settling time and nominal performance recovery for all three controlled areas. We highlight that compared to [53], the proposed algorithm demonstrates better transient performance in accommodating relatively large disturbances. This is an important practical enhancement in ensuring that the stability of the power system is maintained following the occurrence of large load perturbations. It is also evident in this work that the proposed LFC method demonstrates a better steady-state response by minimizing the impact of the lumped disturbance on the controlled output Δf_i, as considered in the controller design. Fig. 5 illustrates the response curve of the disturbance

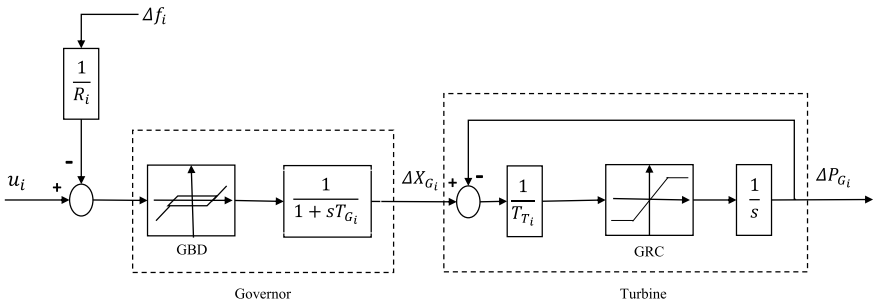

FIGURE 10. Thermal power plant with GRC and GBD nonlinearities [53].

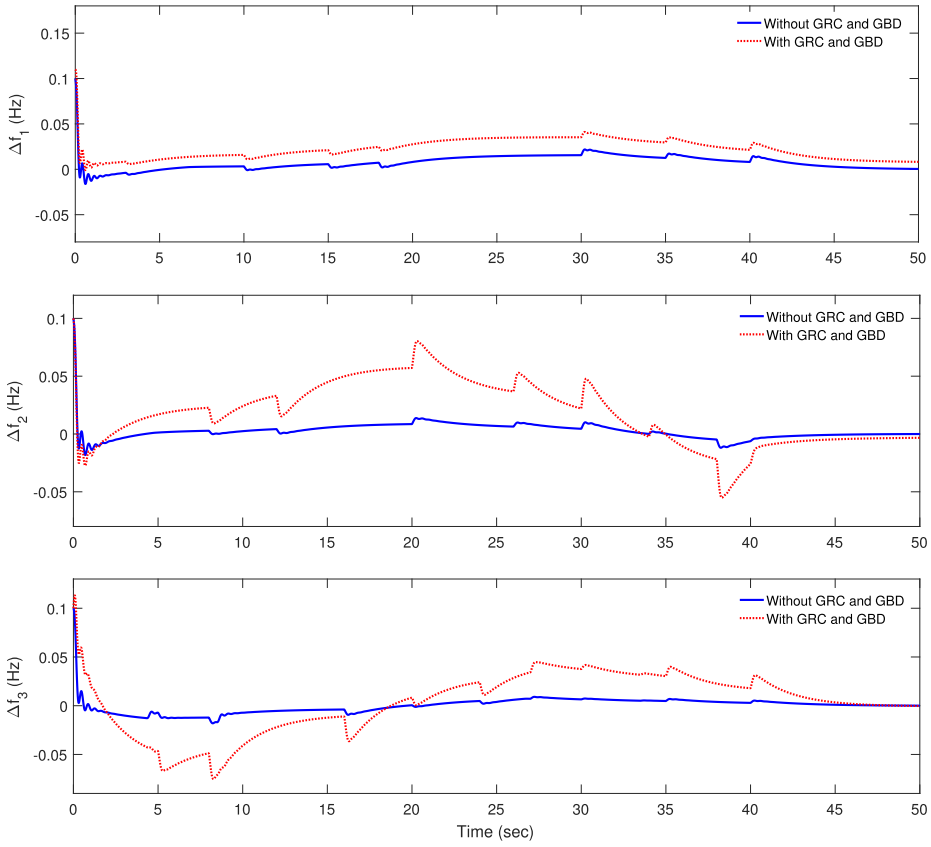

FIGURE 11. Dynamic response of the system frequency Δf_i in all three areas considering GRC and GBD.

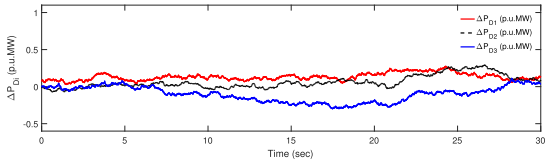

FIGURE 12. Disturbance profile for all three areas including varying step load and wind turbine output power.

estimations for all three areas; the curves show that the estimation errors asymptotically converge to zero.

The sliding surface (13) and control effort (14) for all control areas are shown in Figs. 6 and 7, which show that the system trajectories are driven to the sliding surfaces in all control areas.

Scenario 2: To examine the robustness of the proposed method under real operating conditions, the system performance is evaluated in each controlled area with a lumped disturbance, consisting of varying step load disturbance and system parameter uncertainties. Fig. 8 represents the varying step load disturbance patterns in all three areas. The variations of the system parameters are modeled by the cosine functions, varying $\pm 50\%$ around the nominal values of the system, as listed in Table 1. Fig. 9 shows the dynamic response of system frequency deviations for all control areas. The parameter uncertainties have a minor impact on the frequency

TABLE 3. Performance indices in all controlled areas.

Control Scheme	ISE			IAE			ITAE		
	Controlled Area								
	1	2	3	1	2	3	1	2	3
Proposed method	0.0049	0.0096	0.0195	0.2813	0.3250	0.5974	5.2109	5.4737	10.6326
Synthesis method using Lemma 2	0.0089	0.0208	0.0312	0.3991	0.5765	0.7522	6.7264	10.1303	13.3498
SMLFC [48]	0.0349	0.0490	0.1922	0.7235	0.9520	1.9517	13.8665	17.5444	31.4032
Traditional PI	0.4299	1.6380	2.0010	2.8327	5.3949	6.4936	46.3296	84.4982	91.0595

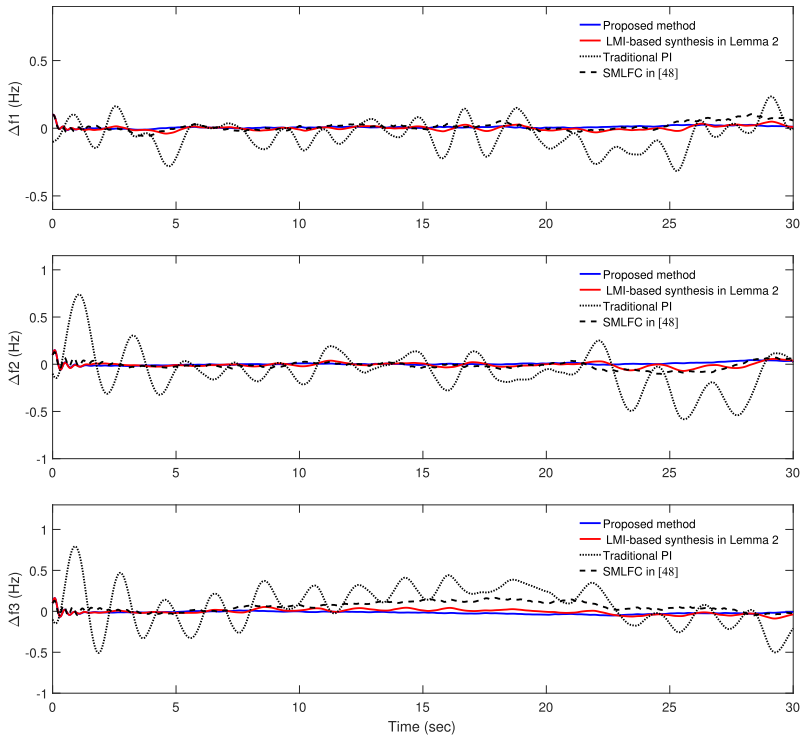

FIGURE 13. Comparative simulation results Δf_i between different control approaches in the presence of random load and wind turbine output power.

performance of the system, thus verifying the robustness of the proposed controller against system parameter uncertainties and load disturbances. Although the effects of nonlinear dynamics are not considered in the design process, nonlinearities such as the GRC and GBD, have been investigated in this simulation; this investigation is important from a practical perspective. The structure of a nonlinear turbine model with a GRC limiter and GBD is depicted in Fig. 10. The GRC value is specified as ± 0.0017p.u.MW/sec for all three areas, where a typical GBD of 0.06% is set for all thermal plants [68].

The simulation results of frequency deviations for different control areas are represented in Fig. 11. The system response exhibits a larger overshoot and longer settling time, but still settles within a permissible range, thereby proving the robust performance of the designed controller.

Scenario 3: This subsection illustrates the effectiveness of the proposed control strategy in handling random disturbances. For the purpose of this simulation, the disturbance $\Delta P_{D_i}(t)$ is constructed by random perturbations as depicted in Fig. 12; the disturbance includes random load variations and wind turbine output power modeled in [69]. The dynamic response Δf_i of the proposed controller is compared with that of the SMLFC in [53] and the conventional PI and LMI-based synthesis method in Lemma 2, as shown in Fig. 13.

The simulation results from Fig. 13 indicate that compared to other control approaches, the proposed method represents superior control performance to remarkably reduce the overshoots of frequency fluctuations in all three controlled areas. A detailed comparison of performance indices is represented in Table 3. Additionally, the proposed method surpasses the method introduced in [53], whereby the frequency deviations in all areas are significantly reduced. Note also that the proposed strategy demonstrates strong robustness to random disturbances, and outperforms other approaches in alleviating the impact of random exogenous disturbances on controlled output Δf_i. This is because the proposed SMC algorithm has been constructed based on the assumption of minimizing the impact of external disturbances on the controlled output.

TABLE 4. Comparative H_∞ performance index $\gamma_i^{\min}$.

Area	Proposed method	Synthesis method using Lemma 2
1	0.4354	0.2478
2	0.2123	0.1014
3	0.3918	0.3075

Furthermore, a summary of the H_∞ performance indices of the proposed framework and the LMI-based synthesis method in Lemma 2 is listed in Table 4. It is evident from Table 4 that compared with the synthesis method in Lemma 2, the proposed scheme obtains a higher H_∞ performance index $\gamma_i^{\min}$ by employing the slack variable in the constructing the LMI in the proposed controller, thereby resulting in better dynamic performance in system frequency deviations.

Thus, the promising results from this simulation highlight the applicability of this approach in overcoming LFC challenges in existing conventional power plants because of random uncertainties caused by renewable energy resources and changes in power consumption patterns.

VI. CONCLUSION

This paper has proposed a decentralized disturbance observer-based sliding mode controller for LFC in a multiarea interconnected power system in the presence of external disturbances, including load variations, output power fluctuations from renewable energy resources and tie-line power deviations. All the external disturbances and uncertainties in the system parameters have been considered to be a lumped disturbance so that the proposed control law is constructed free of tie-line interaction signals, where following this, a reduced order of the system dynamics was derived. A disturbance observer was designed to estimate the lumped disturbance, which was further contained in the design of the integral sliding surface to attenuate the impact of the lumped disturbance on the frequency deviations. The tuning parameters of the sliding surface were obtained based on the H_∞ state feedback control formulated in terms of LMIs. A sliding mode controller was then synthesized to drive the system trajectories onto a region close to the sliding surface in finite time in the presence of lumped disturbance, thus ensuring that the impact of the lumped disturbance on the system frequency is minimized. A three-area power system was used to investigate the effectiveness of the proposed approach. The results have shown that the proposed methodology outperforms other methods in the literature in terms of ease of implementation, dynamic performance, minimizing the effect of the lumped disturbance on power system frequency deviations and increasing the overall lifespan of turbine-generator units in multiarea interconnected power systems.

The penetration of renewable energy sources and the accompanying changes in the electricity market structure and network communication delays in smart grids have increased the challenges of LFC problems in multiarea power systems; consequently, further improvements in the power system frequency performance are required. Motivated by the importance of recent challenges, our future works will be devoted to considering memory-based and higher-order sliding mode controllers in interconnected power systems with communication delays to address the LFC problem.

CREDIT AUTHORSHIP CONTRIBUTION STATEMENT

Farhad Farivar: Conceptualization, Methodology, Software, Validation, Formal analysis. **Octavian Bass:** Supervision, Methodology, Writing - review & editing. **Daryoush Habibi:** Supervision, Methodology, Validation.

DECLARATION OF COMPETING INTERESTS

The authors declare that they have no known competing financial interests or personal relationships that could have appeared to influence the work reported in this paper.

REFERENCES

[1] S. K. Pandey, S. R. Mohanty, and N. Kishor, "A literature survey on load–frequency control for conventional and distribution generation power systems," *Renew. Sustain. Energy Rev.*, vol. 25, pp. 318–334, Sep. 2013.
[2] H. Bevrani, *Robust Power System Frequency Control*. New York, NY, USA: Springer, 2009.
[3] P. Kundur, *Power System Stability and Control*. New York, NY, USA: McGraw-Hill, 1994.
[4] C. K. Das, O. Bass, G. Kothapalli, T. S. Mahmoud, and D. Habibi, "Overview of energy storage systems in distribution networks: Placement, sizing, operation, and power quality," *Renew. Sustain. Energy Rev.*, vol. 91, pp. 1205–1230, Aug. 2018.
[5] D. Wang, L. Liu, H. Jia, W. Wang, Y. Zhi, Z. Meng, and B. Zhou, "Review of key problems related to integrated energy distribution systems," *CSEE J. Power Energy Syst.*, vol. 4, no. 2, pp. 130–145, Jun. 2018.
[6] M. Elsisi, N. Bazmohammadi, J. M. Guerrero, and M. A. Ebrahim, "Energy management of controllable loads in multi-area power systems with wind power penetration based on new supervisor fuzzy nonlinear sliding mode control," *Energy*, vol. 221, Apr. 2021, Art. no. 119867.
[7] X.-C. Shangguan, C.-K. Zhang, Y. He, L. Jin, L. Jiang, J. W. Spencer, and M. Wu, "Robust load frequency control for power system considering transmission delay and sampling period," *IEEE Trans. Ind. Informat.*, vol. 17, no. 8, pp. 5292–5303, Aug. 2021.
[8] Y. Sun, N. Li, X. Zhao, Z. Wei, G. Sun, and C. Huang, "Robust H_∞ load frequency control of delayed multi-area power system with stochastic disturbances," *Neurocomputing*, vol. 193, pp. 58–67, Jun. 2016.
[9] H. Bevrani and T. Hiyama, "Robust decentralised PI based LFC design for time delay power systems," *Energy Convers. Manag.*, vol. 49, no. 2, pp. 193–204, Feb. 2008.
[10] E. Çam and İ. Kocaarslan, "A fuzzy gain scheduling PI controller application for an interconnected electrical power system," *Electr. Power Syst. Res.*, vol. 73, no. 3, pp. 267–274, Mar. 2005.
[11] M. Elsisi, M. Soliman, M. A. S. Aboelela, and W. Mansour, "ABC based design of PID controller for two area load frequency control with nonlinearities," *TELKOMNIKA Indonesian J. Electr. Eng.*, vol. 16, no. 1, pp. 58–64, 2015.
[12] F. Daneshfar and H. Bevrani, "Multiobjective design of load frequency control using genetic algorithms," *Int. J. Electr. Power Energy Syst.*, vol. 42, no. 1, pp. 257–263, Nov. 2012.
[13] K. Naidu, H. Mokhlis, and A. H. A. Bakar, "Multiobjective optimization using weighted sum artificial bee colony algorithm for load frequency control," *Int. J. Electr. Power Energy Syst.*, vol. 55, pp. 657–667, Feb. 2014.
[14] M. Rahmani and N. Sadati, "Two-level optimal load–frequency control for multi-area power systems," *Int. J. Electr. Power Energy Syst.*, vol. 53, pp. 540–547, Dec. 2013.
[15] K. P. S. Parmar, S. Majhi, and D. P. Kothari, "Load frequency control of a realistic power system with multi-source power generation," *Int. J. Electr. Power Energy Syst.*, vol. 42, no. 1, pp. 426–433, Nov. 2012.

[16] S. Velusami and K. Romar, "Design of observer-based decentralized load-frequency controllers for interconnected power systems," *Int. J. Power Energy Syst.*, vol. 17, no. 2, pp. 152–160, 1997.

[17] K. Yamashita and T. Taniguchi, "Optimal observer design for load-frequency control," *Int. J. Electr. Power Energy Syst.*, vol. 8, no. 2, pp. 93–100, Apr. 1986.

[18] N. Hasan, I. Nasiruddin, P. Kumar, and N. Hakimuddin, "Sub-optimal automatic generation control of interconnected power system using constrained feedback control strategy," *Int. J. Electr. Power Energy Syst.*, vol. 43, no. 1, pp. 295–303, Dec. 2012.

[19] A. Rubaai and V. Udo, "An adaptive control scheme for load-frequency control of multiarea power systems. Part I. Identification and functional design," *Electr. Power Syst. Res.*, vol. 24, no. 3, pp. 183–188, Sep. 1992.

[20] I. Vajk, M. Vajta, L. Keviczky, R. Haber, J. Hetthéssy, and K. Kovács, "Adaptive load-frequency control of the Hungarian power system," *Automatica*, vol. 21, no. 2, pp. 129–137, Mar. 1985.

[21] R. R. Shoults and J. J. Ibarra, "Multi-area adaptive LFC developed for a comprehensive AGC simulator," *IEEE Trans. Power Syst.*, vol. 8, no. 2, pp. 541–547, May 1993.

[22] M.-H. Khooban, T. Niknam, F. Blaabjerg, P. Davari, and T. Dragicevic, "A robust adaptive load frequency control for micro-grids," *ISA Trans.*, vol. 65, pp. 220–229, Nov. 2016.

[23] T. H. Mohamed, M. A. M. Alamin, and A. M. Hassan, "A novel adaptive load frequency control in single and interconnected power systems," *Ain Shams Eng. J.*, vol. 12, no. 2, pp. 1763–1773, Jun. 2021.

[24] K. R. Sudha and R. V. Santhi, "Load frequency control of an interconnected reheat thermal system using type-2 fuzzy system including SMES units," *Int. J. Electr. Power Energy Syst.*, vol. 43, no. 1, pp. 1383–1392, Dec. 2012.

[25] H. Yousef, "Adaptive fuzzy logic load frequency control of multi-area power system," *Int. J. Electr. Power Energy Syst.*, vol. 68, pp. 384–395, Jun. 2015.

[26] İ. Kocaarslan and E. Çam, "Fuzzy logic controller in interconnected electrical power systems for load-frequency control," *Int. J. Electr. Power Energy Syst.*, vol. 27, no. 8, pp. 542–549, Oct. 2005.

[27] K. R. Sudha and R. V. Santhi, "Robust decentralized load frequency control of interconnected power system with generation rate constraint using type-2 fuzzy approach," *Int. J. Electr. Power Energy Syst.*, vol. 33, no. 3, pp. 699–707, Mar. 2011.

[28] K. R. Sudha, Y. B. Raju, and A. C. Sekhar, "Fuzzy C-means clustering for robust decentralized load frequency control of interconnected power system with generation rate constraint," *Int. J. Electr. Power Energy Syst.*, vol. 37, no. 1, pp. 58–66, May 2012.

[29] T. H. Mohamed, H. Bevrani, A. A. Hassan, and T. Hiyama, "Decentralized model predictive based load frequency control in an interconnected power system," *Energy Convers. Manag.*, vol. 52, no. 2, pp. 1208–1214, 2011.

[30] M. Ma, H. Chen, X. Liu, and F. Allgöwer, "Distributed model predictive load frequency control of multi-area interconnected power system," *Int. J. Electr. Power Energy Syst.*, vol. 62, pp. 289–298, Nov. 2014.

[31] Y. Zheng, J. Zhou, Y. Xu, Y. Zhang, and Z. Qian, "A distributed model predictive control based load frequency control scheme for multi-area interconnected power system using discrete-time Laguerre functions," *ISA Trans.*, vol. 68, pp. 127–140, May 2017.

[32] M. Elsisi, M. Aboelela, M. Soliman, and W. Mansour, "Design of optimal model predictive controller for LFC of nonlinear multi-area power system with energy storage devices," *Electr. Power Compon. Syst.*, vol. 46, nos. 11–12, pp. 1300–1311, Jul. 2018.

[33] H. Bevrani, Y. Mitani, and K. Tsuji, "Robust decentralised load-frequency control using an iterative linear matrix inequalities algorithm," *IEE Proc., Gener. Transmiss. Distrib.*, vol. 151, no. 3, pp. 347–354, May 2004.

[34] D. Rerkpreedapong, A. Hasanovic, and A. Feliachi, "Robust load frequency control using genetic algorithms and linear matrix inequalities," *IEEE Trans. Power Syst.*, vol. 18, no. 2, pp. 855–861, May 2003.

[35] X. Yu and K. Tomsovic, "Application of linear matrix inequalities for load frequency control with communication delays," *IEEE Trans. Power Syst.*, vol. 19, no. 3, pp. 1508–1515, Aug. 2004.

[36] K. Lu, W. Zhou, G.-Q. Zeng, and Y. Zheng, "Constrained population extremal optimization-based robust load frequency control of multi-area interconnected power system," *Int. J. Electr. Power Energy Syst.*, vol. 105, pp. 249–271, Feb. 2019.

[37] Z. M. Al-Hamouz and H. N. Al-Duwaish, "A new load frequency variable structure controller using genetic algorithms," *Electr. Power Syst. Res.*, vol. 55, no. 1, pp. 1–6, Jul. 2000.

[38] O. P. Malik, A. Kumar, and G. S. Hope, "A load frequency control algorithm based on a generalized approach," *IEEE Trans. Power Syst.*, vol. PWRS-3, no. 2, pp. 375–382, May 1988.

[39] Z. M. Al-Hamouz and Y. L. Abdel-Magid, "Variable structure load frequency controllers for multiarea power systems," *Int. J. Electr. Power Energy Syst.*, vol. 15, no. 5, pp. 293–300, Jan. 1993.

[40] A. Y. Sivaramakrlshnan, M. V. Hariharan, and M. C. Srisailam, "Design of variable-structure load-frequency controller using pole assignment technique," *Int. J. Control*, vol. 40, no. 3, pp. 487–498, 1984.

[41] K. R. M. V. Chandrakala, S. Balamurugan, and K. Sankaranarayanan, "Variable structure fuzzy gain scheduling based load frequency controller for multi source multi area hydro thermal system," *Int. J. Electr. Power Energy Syst.*, vol. 53, pp. 375–381, Dec. 2013.

[42] H. Shayeghi, H. A. Shayanfar, and A. Jalili, "Load frequency control strategies: A state-of-the-art survey for the researcher," *Energy Convers. Manag.*, vol. 50, no. 2, pp. 344–353, Feb. 2009.

[43] R. Shankar, S. R. Pradhan, K. Chatterjee, and R. Mandal, "A comprehensive state of the art literature survey on LFC mechanism for power system," *Renew. Sustain. Energy Rev.*, vol. 76, pp. 1185–1207, Sep. 2017.

[44] J. Guo, "Application of full order sliding mode control based on different areas power system with load frequency control," *ISA Trans.*, vol. 92, pp. 23–34, Sep. 2019.

[45] Y. Cui, L. Xu, M. Fei, and Y. Shen, "Observer based robust integral sliding mode load frequency control for wind power systems," *Control Eng. Pract.*, vol. 65, pp. 1–10, Aug. 2017.

[46] D. Qian, S. Tong, H. Liu, and X. Liu, "Load frequency control by neural-network-based integral sliding mode for nonlinear power systems with wind turbines," *Neurocomputing*, vol. 173, pp. 875–885, Jan. 2016.

[47] C. Mu, Y. Tang, and H. He, "Improved sliding mode design for load frequency control of power system integrated an adaptive learning strategy," *IEEE Trans. Ind. Electron.*, vol. 64, no. 8, pp. 6742–6751, Aug. 2017.

[48] V. I. Utkin and H.-C. Chang, "Sliding mode control on electro-mechanical systems," *Math. Problems Eng.*, vol. 8, nos. 4–5, pp. 451–473, 2002.

[49] K. D. Young, V. I. Utkin, and U. Ozguner, "A control engineer's guide to sliding mode control," *IEEE Trans. Control Syst. Technol.*, vol. 7, no. 3, pp. 328–342, May 1999.

[50] S. Prasad, S. Purwar, and N. Kishor, "Non-linear sliding mode load frequency control in multi-area power system," *Control Eng. Pract.*, vol. 61, pp. 81–92, Apr. 2017.

[51] S. Prasad, S. Purwar, and N. Kishor, "Load frequency regulation using observer based non-linear sliding mode control," *Int. J. Electr. Power Energy Syst.*, vol. 104, pp. 178–193, Jan. 2019.

[52] K. Vrdoljak, N. Perić, and I. Petrović, "Sliding mode based load-frequency control in power systems," *Electr. Power Syst. Res.*, vol. 80, no. 5, pp. 514–527, 2010.

[53] Y. Mi, Y. Fu, C. Wang, and P. Wang, "Decentralized sliding mode load frequency control for multi-area power systems," *IEEE Trans. Power Syst.*, vol. 28, no. 4, pp. 4301–4309, Nov. 2013.

[54] M. Elsisi and H. Abdelfattah, "New design of variable structure control based on lightning search algorithm for nuclear reactor power system considering load-following operation," *Nucl. Eng. Technol.*, vol. 52, no. 3, pp. 544–551, Mar. 2020.

[55] H. Li, X. Wang, and J. Xiao, "Adaptive event-triggered load frequency control for interconnected microgrids by observer-based sliding mode control," *IEEE Access*, vol. 7, pp. 68271–68280, 2019.

[56] Z. Wu, H. Mo, J. Xiong, and M. Xie, "Adaptive event-triggered observer-based output feedback $\mathcal{L}_\infty$ load frequency control for networked power systems," *IEEE Trans. Ind. Informat.*, vol. 16, no. 6, pp. 3952–3962, Jun. 2020.

[57] J. Hu, H. Zhang, H. Liu, and X. Yu, "A survey on sliding mode control for networked control systems," *Int. J. Syst. Sci.*, vol. 52, no. 6, pp. 1129–1147, Apr. 2021.

[58] K. Liao and Y. Xu, "A robust load frequency control scheme for power systems based on second-order sliding mode and extended disturbance observer," *IEEE Trans. Ind. Informat.*, vol. 14, no. 7, pp. 3076–3086, Jul. 2018.

[59] Y. Mi, Y. Fu, D. Li, C. Wang, P. C. Loh, and P. Wang, "The sliding mode load frequency control for hybrid power system based on disturbance observer," *Int. J. Electr. Power Energy Syst.*, vol. 74, pp. 446–452, Jan. 2016.

[60] A. Ahmadi and M. Aldeen, "An LMI approach to the design of robust delay-dependent overlapping load frequency control of uncertain power systems," *Int. J. Electr. Power Energy Syst.*, vol. 81, pp. 48–63, Oct. 2016.

[61] L. Xiong, H. Li, and J. Wang, "LMI based robust load frequency control for time delayed power system via delay margin estimation," *Int. J. Electr. Power Energy Syst.*, vol. 100, pp. 91–103, Sep. 2018.
[62] M. Hamzeh, S. Emamian, H. Karimi, and J. Mahseredjian, "Robust control of an islanded microgrid under unbalanced and nonlinear load conditions," *IEEE Trans. Emerg. Sel. Topics Power Electron.*, vol. 4, no. 2, pp. 512–520, Jun. 2016.
[63] V. P. Singh, N. Kishor, and P. Samuel, "Improved load frequency control of power system using LMI based PID approach," *J. Franklin Inst.*, vol. 354, no. 15, pp. 6805–6830, Oct. 2017.
[64] S. Prasad, S. Purwar, and N. Kishor, "On design of a non-linear sliding mode load frequency control of interconnected power system with communication time delay," in *Proc. IEEE Conf. Control Appl. (CCA)*, Sep. 2015, pp. 1546–1551.
[65] G.-R. Duan and H.-H. Yu, *LMIs in Control Systems: Analysis, Design and Applications*. Boca Raton, FL, USA: CRC Press, 2013.
[66] P. Haghighi, B. Tavassoli, and A. Farhadi, "A practical approach to networked control design for robust H_∞ performance in the presence of uncertainties in both communication and system," *Appl. Math. Comput.*, vol. 381, Sep. 2020, Art. no. 125308.
[67] J. Löfberg, "Automatic robust convex programming," *Optim. Methods Softw.*, vol. 27, no. 1, pp. 115–129, Sep. 2012.
[68] P. Bhui, N. Senroy, A. K. Singh, and B. C. Pal, "Estimation of inherent governor dead-band and regulation using unscented Kalman filter," *IEEE Trans. Power Syst.*, vol. 33, no. 4, pp. 3546–3558, Jul. 2018.
[69] M. Takagi, K. Yamaji, and H. Yamamoto, "Power system stabilization by charging power management of plug-in hybrid electric vehicles with LFC signal," in *Proc. IEEE Vehicle Power Propuls. Conf.*, Sep. 2009, pp. 822–826.
[70] H. Khalil, *Nonlinear Control*. New York, NY, USA: Pearson, 2015.

FARHAD FARIVAR (Graduate Student Member, IEEE) received the B.S. degree in electrical power systems from Azad University, Iran, in 2006, and the M.Eng. degree in instrumentation, control, and automation from Edith Cowan University, Joondalup, WA, Australia, in 2014, where he is currently pursuing the Ph.D. degree with the Smart Energy Systems Group. Since 2014, he has been a Senior Automation, Control, and Power Engineer with the School of Engineering, Edith Cowan University. His main research interest includes applications of control theories in power systems.

OCTAVIAN BASS (Senior Member, IEEE) received the bachelor's and Ph.D. degrees from the Politehnica University of Timisoara, Romania, in 1995 and 2001, respectively. His employment history includes research positions with the Budapest University of Technology and Economics, Hungary; The Hong Kong Polytechnic University; Hull University, U.K.; and Utsunomiya University, Japan. He was a Lecturer with James Cook University, Australia, from 2006 to 2009. He is currently a Senior Lecturer with the School of Engineering, Edith Cowan University, Perth, WA, Australia. He has coauthored 90 professional publications. His research interests include smart grid technologies, renewable energy resources, and nonlinear dynamics in power electronic

DARYOUSH HABIBI (Senior Member, IEEE) received the B.E. degree (Hons.) in electrical engineering and the Ph.D. degree from the University of Tasmania, Hobart, TAS, Australia, in 1989 and 1994, respectively. His employment history includes Telstra Research Laboratories, Flinders University, Intelligent Pixels Inc., and Edith Cowan University, Joondalup, WA, Australia, where he is currently a Professor, the Pro Vice-Chancellor, and the Executive Dean of the School of Engineering. His research interests include engineering design for sustainable development, reliability and quality of service in communication systems and networks, smart energy systems, and environmental monitoring technologies. He is a fellow of Engineers Australia and the Institution for Marine Engineering, Science and Technology.